Photodiagnosis and Photodynamic Therapy 33 (2021) 102173

Contents lists available at ScienceDirect

Photodiagnosis and Photodynamic Therapy

journal homepage: www.elsevier.com/locate/pdpdt

The synergistic effect of focused ultrasound and biophotonics to overcome the barrier of light transmittance in biological tissue

Jaehyuk Kim [a,b], Jaewoo Shin [c], Chanho Kong [c], Sung-Ho Lee [a], Won Seok Chang [c], Seung Hee Han [a,d,*]

[a] Molecular Imaging, Princess Margaret Cancer Centre, Toronto, ON, Canada
[b] Health and Medical Equipment, Samsung Electronics Co. Ltd., Suwon, Republic of Korea
[c] Department of Neurosurgery, Brain Research Institute, Yonsei University College of Medicine, Seoul, Republic of Korea
[d] Department of Medical Biophysics, University of Toronto, Toronto, ON, Canada

ARTICLE INFO

Keywords:
Light transmission enhancement
Focused Ultrasound
Air bubble
Mechanical deformation
Rat brain

ABSTRACT

Optical technology is a tool to diagnose and treat human diseases. Shallow penetration depth caused by the high optical scattering nature of biological tissues is a significant obstacle to utilizing light in the biomedical field. In this paper, light transmission enhancement in the rat brain induced by focused ultrasound (FUS) was observed and the cause of observed enhancement was analyzed. Both air bubbles and mechanical deformation generated by FUS were cited as the cause. The Monte Carlo simulation was performed to investigate effects on transmission by air bubbles and finite element method was also used to describe mechanical deformation induced by motions of acoustic particles. As a result, it was found that the mechanical deformation was more suitable to describe the transmission change according to the FUS pulse observed in the experiment.

1. Introduction

Optical technology in the biomedical field has many possibilities. This technology is relatively free of overdose-related problems compared to other technologies such as CT and PET, and is sensitive to soft tissue compared to ultrasound-based technology. However, optical technology has a fatal limitation produced by the nature of light. Delivering optical photons to the deep biological tissue is one of the main objectives for bio-optical imaging and treatment technique.

Conventionally, scattering of light caused by the heterogeneous optical properties of biological tissues limit the penetration ability of optical photons. To overcome this limitation, many studies combining ultrasound technology and optical methods have been reported. For example, photoacoustic technology has solved this limitation by converting scattered and non-ballistic light photons into non-scattering ultrasound waves. Researchers also have been trying to use ultrasound technology as a tagging method in diffuse optical tomography [1]. Unlike these research focused on detecting efficiency, there have been research to increase light delivery itself [2–7]. These kinds of methods are based on feedback between scattered light inside the tissue and the incident wavefront. Ultrasound, photoacoustic and non-linear photoacoustic are used as a method for feedback. As a result, modulated incident photons are gathered at the region of interest.

Other researchers have been trying to modulate optical properties of biological tissues. The optical properties of biological tissues are described in terms of parameters related with absorption (the absorption coefficient) and scattering (the scattering coefficient and the anisotropy of scatter) [8]. The anisotropy of scatter represents features of tissue scattering in terms of the relative forward versus backward direction of scatter. Raymond et al. has studied the relationship between the optical properties modulated by high intensity focused ultrasound and the transmission of light [9]. Recently, a more intuitive and simple study by Kim et al. showed that irradiation of focused ultrasound inside tissues could increase light penetration in the tissues [10]. They insisted that air bubbles generated by focused ultrasound energy within the focal area turns biological tissue into a Mie scattering dominant medium. Since Mie scattering has a high forward-dominant scattering pattern, more incident light can reach directly into deep tissue. However, because the values of the anisotropy of scatter in biological tissue are more than 0.8 at visible wavelength [11], it seems that Mie scattering already occurs frequently in the biological tissue. Therefore, we predicted that there should be some other elements to explain the increase of light

* Corresponding author at: 15th floor, Molecular imaging, Princess Margaret Cancer Centre, 101 college street, Toronto, ON, Canada, M5G 1L7
E-mail address: Han.HeeSeung@uhnresearch.ca (S.H. Han).

https://doi.org/10.1016/j.pdpdt.2020.102173
Received 1 August 2020; Received in revised form 9 December 2020; Accepted 23 December 2020
Available online 30 January 2021

Fig. 1. Blood-eliminated rat brain.

penetration by FUS.

The interaction of ultrasound with tissue can be classified into two categories – thermal and non-thermal procedures. Thermal effects are related to direct absorption of the ultrasound energy and converting absorbed energy into heat. Acoustic radiation force, radiation torque, acoustic streaming, shockwave and cavitation belong to non-thermal effects [12]. When mechanical pressure caused by acoustic force is applied to biological tissue, the target tissue is displaced. Typically, this displacement is only in the axial direction. However, because most biological tissues are nearly incompressible, axial displacement makes tissues expand in the lateral direction [13,14].

Photodynamic therapy (PDT) is one of the most popular optical treatment technologies used for cancer treatment. The recent approval of 5-aminolevulinic acid (5-ALA) by the United States Food and Drug Administration (FDA) raised interests in leveraging this agent as a means to PDT. In the case of brain cancer, more than 80% of recurrences are located adjacent to the resection cavity. In principle, PDT to the resection cavity can minimize the risk of local recurrence [15]. Focused ultrasound (FUS) technology is also a highly promising treatment for brain disease such as Parkinson's disease. Currently, treatment using FUS has mainly used a method based on thermal ablation. However, other methods such as drug delivery through the blood-brain barrier (BBB) opening has been studied recently [16]. Therefore, FUS has the potential to efficiently deliver agents for brain PDT, and has the ability to overcome the limitation of light penetration. In order to take full advantage of these novel methods and technologies, the mechanism behind both the advantage and limitation must be properly understood. In this paper, we observe a FUS assisted enhancement of light transmission in the rat brain and calculate the influence of mechanical deformation by acoustic force and air bubbles on enhancement in biological tissue.

2. Methods and materials

2.1. Experimental setup

To validate a FUS assisted enhancement of light transmission in rat brain, a FUS-combined light irradiation system was constructed. A continuous wave (CW) laser diode with wavelength 637 nm (LP637-SF70, Thorlabs Inc.) was used as a light source for the system. Output light from the end of the fiber coupled with laser diode was collimated by using a collimator (F260FC-B, Thorlabs Inc.). A compact laser diode controller (CLD1010LP, Thorlabs Inc.) was responsible for turning on and off the laser diode. It also adjusted the output power and the temperature of the laser diode. The pulsed FUS was generated from a ring-shape transducer with a frequency of 0.515 MHz, a diameter of 63.2 mm and a radius of curvature of 63.2 mm (H107, Sonic Concept Inc.). As a driving equipment for the transducer, a waveform generator (33220A, Agilent) which was connected to a 50-dB Radio Frequency Power Amplifier (240 L, ENI Inc.) was used. The impedance of transducer and amplifier was matched by using an external matching network (Sonic Concept Inc.). The transducer was mounted on a cone filled with degassed water, and the end of its tip was wrapped in a polyurethane membrane. The degassed water was circulated by water circulation device. Peak pressure was varied from 2.2 to 4.175 MPa corresponding to the value from 76.66 to 270 W/cm^2. The burst pulse repetition rate was 1 Hz and the duty cycle was 50%. The transmission image was captured by a smartphone camera (Galaxy Note 9, Samsung Electronics). The "expert mode" was used to keep the parameters of a camera such as ISO, shutter speed, etc.

To restrict the observations of the symptoms to the brain tissue, a rat brain was extracted and blood inside the brain was flushed out using saline. An ultrasonic gel covered the gap between the cone and the rat brain (Figs. 1 and 2).

2.2. Monte-Carlo simulation

Changes in distribution of optical photon according to the existence

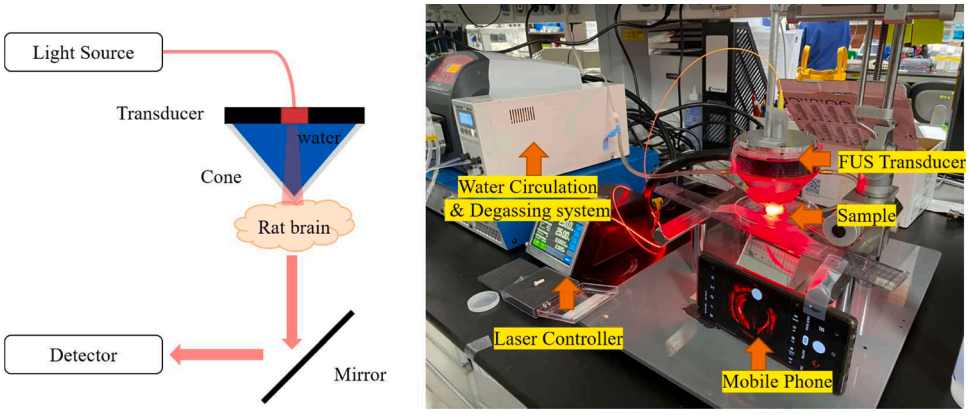

Fig. 2. Experimental setup.

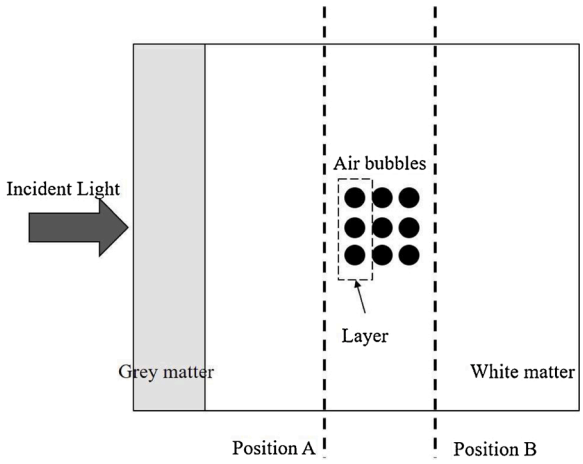

Fig. 3. Simulated structure.

Table 1
Optical properties of simulated materials.

	n	L_a (mm)	L_s (mm)	g_f	r
White matter	1.46	12.5	0.024	0.87	1
Gray matter	1.46	50	0.11	0.89	1
Air bubble	1	–	–	–	–

of air bubbles inside a brain tissue were calculated by using a Monte Carlo (MC) simulation. An open source library, GEANT4 (Geometry ANd Tracking) which can simulate the passage of particles through the matter, was selected as an engine of our Monte Carlo Simulation [17]. Dubois et al. carried out GEANT4 based MC simulation to optimize the design of optode to perform optogenetic modulation [18]. In our simulation model, an EMPhysics_op4 class was applied as a physical engine. Absorption, Mie scattering, Rayleigh scattering, refraction and reflection at boundaries were included. The refractive index (n), absorption length (L_a), scattering length (L_s) and forward-scattering anisotropy (g_f), backward scattering anisotropy (g_b) and the ratio between forward and backward scattering (r) are defined for each structure [19]. The calculation of Mie scattering follows the Henyey–Greenstein approximation with the forward and backward angles treated separately. L_a and L_s are defined as follows:

$$L_a = \frac{1}{\mu_a}, \quad L_s = \frac{1-g}{\mu_s'} \tag{1}$$

The differential cross-section is defined by using g_a, g_f and r as follows [20]:

$$\frac{d\sigma}{d\Omega} = r\frac{d\sigma}{d\Omega}(\theta_f, \ g_f) + (1-r)\frac{d\sigma}{d\Omega}(\theta_b, \ g_b) \tag{2}$$

Simulated structure is shown in Fig. 3. Thicknesses of grey and white matter are 1 cm and 100 μm, respectively. Air bubbles (diameters of 50–200 μm) inside white matter, 5 layers, and 10 μm gaps between bubbles were modeled. Number of light photons passed through planes located in position A and B were recorded. Materials and Optical properties of each material used in our Monte Carlo simulation are summarized in Table 1 [21].

2.3. Elastic wave simulation

As mentioned above, when FUS is applied on biological tissue, both compressional and shear wave can exist. The propagation of compressional and shear wave can be described using Hooke's law and the conservation of momentum. In biological tissues, Hooke's law is extended to the stress-strain relation. The Kelvin-Voigt model is widely used for calculating the elastic behavior of viscoelastic materials:

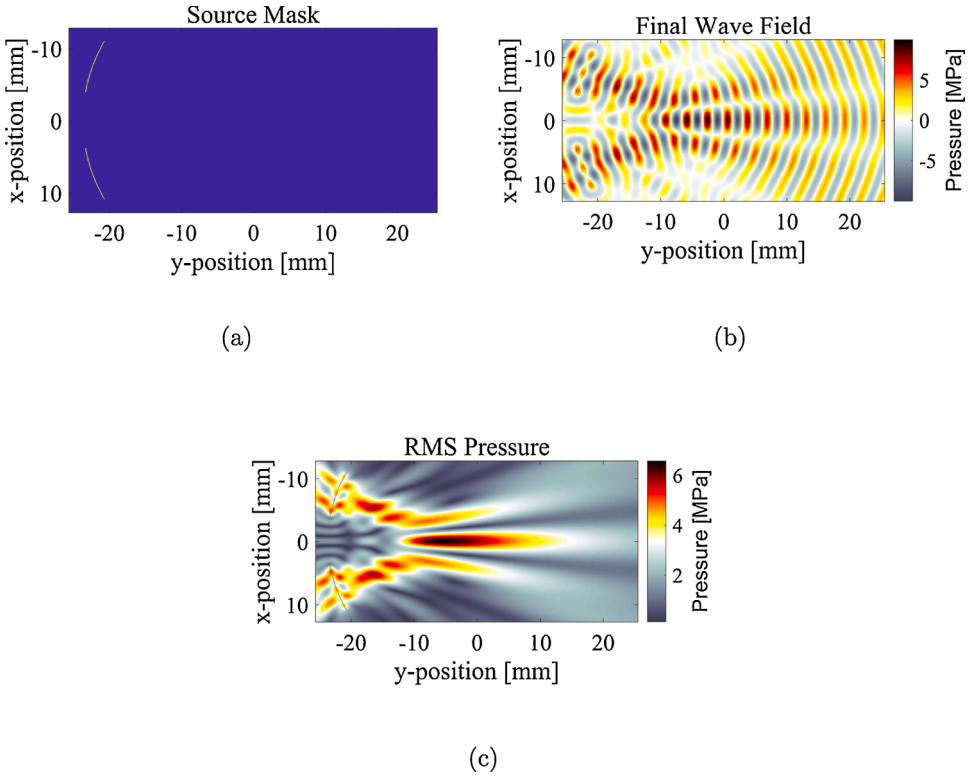

Fig. 4. (a) shape of modeled source (yellow line), (b) wave field generated by source, and (c) RMS pressure applied on media.

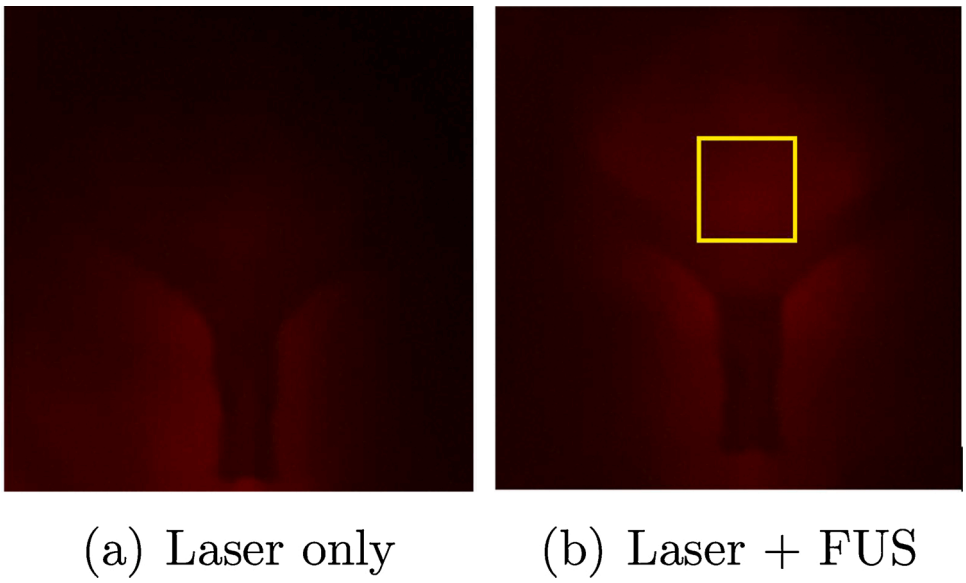

Fig. 5. Change in light transmission pattern in the rat brain according to the existence of FUS irradiation.

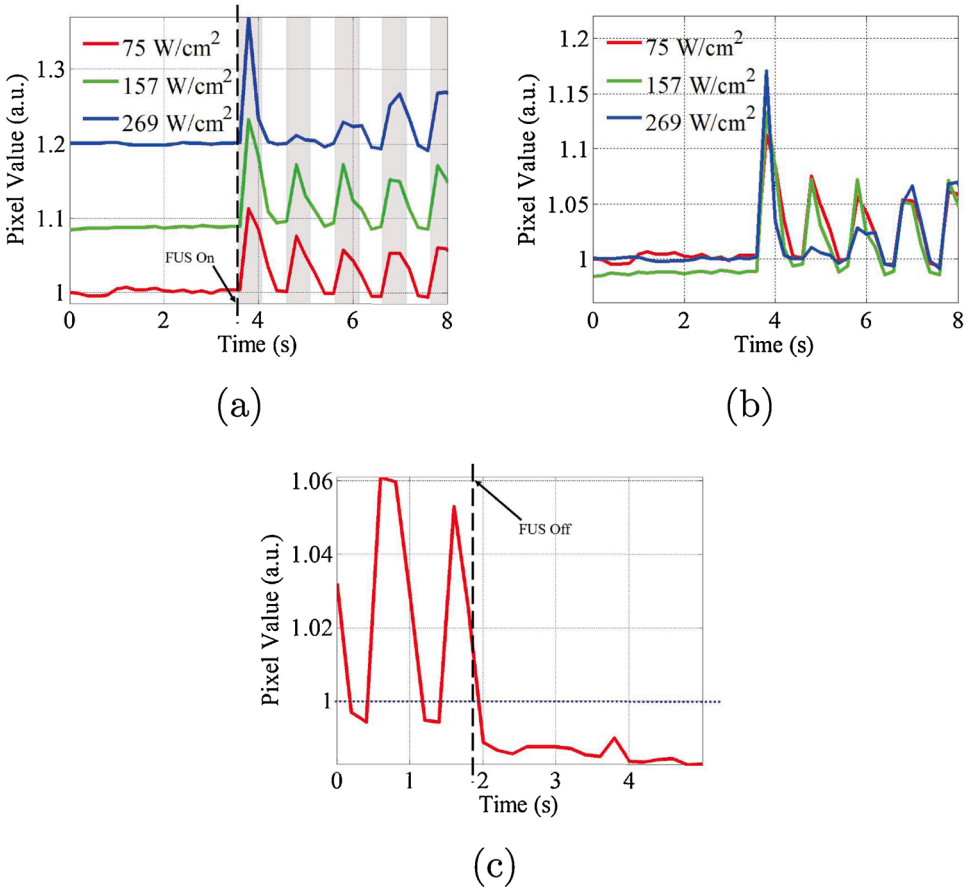

Fig. 6. Changes in averaged pixel value at focal point. (a) Average intensity variation when starting to FUS signal. Shaded area indicates FUS pulse irradiation period, (b) intensity variation normalized by intensity before FUS irradiation of 75 W/cm^2, and (c) intensity change over time after FUS off (75 W/cm^2).

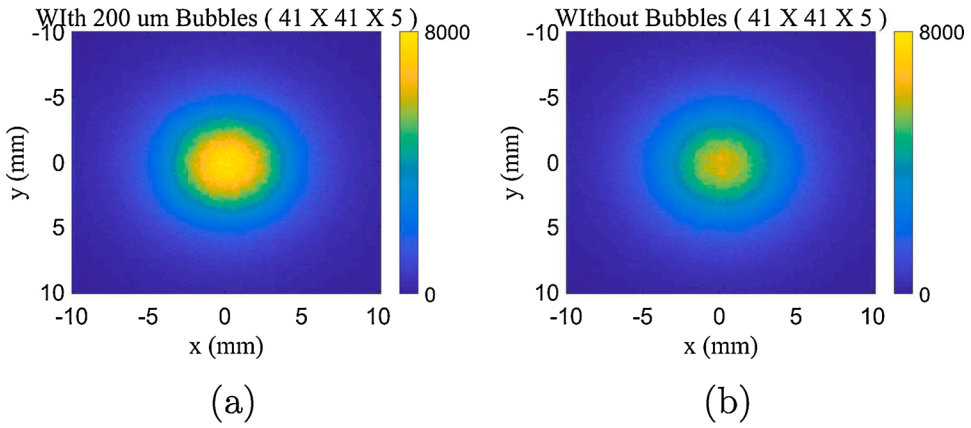

Fig. 7. The number of photons passed through a plane located at position A: (a) with air bubbles and (b) without bubbles.

$$\frac{\partial \sigma_{ij}}{\partial t} = \lambda \delta_{ij} \frac{\partial \nu_k}{\partial x_k} + \mu \left(\frac{\partial \nu_i}{\partial x_j} + \frac{\partial \nu_j}{\partial x_i} \right) + \chi \delta_{ij} \frac{\partial^2 \nu_k}{\partial x_k \partial t} + \eta \left(\frac{\partial^2 \nu_i}{\partial x_j \partial t} + \frac{\partial^2 \nu_j}{\partial x_i \partial t} \right) \tag{3}$$

$$\frac{\partial \nu_i}{\partial t} = \frac{1}{\rho} \frac{\partial \sigma_{ij}}{\partial x_i} \tag{4}$$

Here, σ is the stress tensor, μ and λ are the Lame parameters, ν is the particle velocity and χ and η are the compressional and shear viscosity coefficients. The open source k-wave toolbox can solve elastic wave equation described above [22].

Because of the limitation of computing power, a two-dimensional simulation was performed. Fig. 4(a)–(c) shows a shape of ultrasound source, wave pattern, and distribution of calculated RMS pressure, respectively. Inner and outer radius of source are 64 and 22.6 mm. The radius of curvature is 63.2 mm and source frequency is 0.515 MHz. All values of the transducer used in this experiment is the value of H107. An isotropic medium with density 1046 kg/m^3 and sound speed 1552 m/s was assumed. For simplicity, all types of absorption were ignored.

3. Results

Fig. 5 shows acquired rat brain images. The focal point of FUS is located slightly above the center of the images. When FUS was not applied (Fig. 5(a)), incident light was dramatically scattered by brain tissues and most of the transmitted light was observed near crevices in the brain. However, when FUS was applied (Fig. 5(b)), the amount of light transmitted through the brain tissue was increased. FUS with peak pressure from 2.2 to 4.175 MPa corresponding to the value of averaged ultrasound intensities from 76.66 to 269 W/cm^2 was applied. Burst pulse was applied once per second and the length of the burst pulse was 500 ms. To measure changes in light transmission in the time domain, images of the brain were acquired at a speed of 30 fps. Region of interest (ROI) was set around the focal point of the FUS as shown in Fig. 5(b). Pixel values inside ROI were accumulated, normalized with background signal, and plotted in Fig. 6. It was observed that the intensity increased abruptly as soon as the first FUS pulse was applied. In contrast, from the second FUS pulse, the increase fluctuated in the direction of reduction. Note that FUS pulses were applied with frequency 1 Hz. To analyze these changes in light transmission, two types of simulation were performed.

Cavitation air bubbles were the first variable to consider. Unfortunately, it is hard to measure the size and number of actual microbubbles inside brain tissue. Also the rheological applications are relatively unexplored. What we know is acoustic induced cavitation produces a group of microbubbles and owing to its collective characteristics, a threshold of the cavitation was reported [23]. Therefore, parameters that fit the assumptions about the role of air bubbles were selected. According to the paper by Kim et al. [10], the main role of air bubbles that leads to light enhancement, is the generation of the forward scattering pattern. To make a forward scattering, scattering by air bubbles must be the Mie scattering. If the bubble sizes were sufficiently large, it could result in Mie scattering with a high forward scattering rate. And because the refractive index inside the air bubble ($n = 1$) was different from the surrounding biological material, air bubbles could affect the scattering pattern inside biological media, in our case, the brain. The type of scattering according to the bubble size can be easily predicted with a parameter called size parameter, x, if we assume that the bubbles are shaped as spheres:

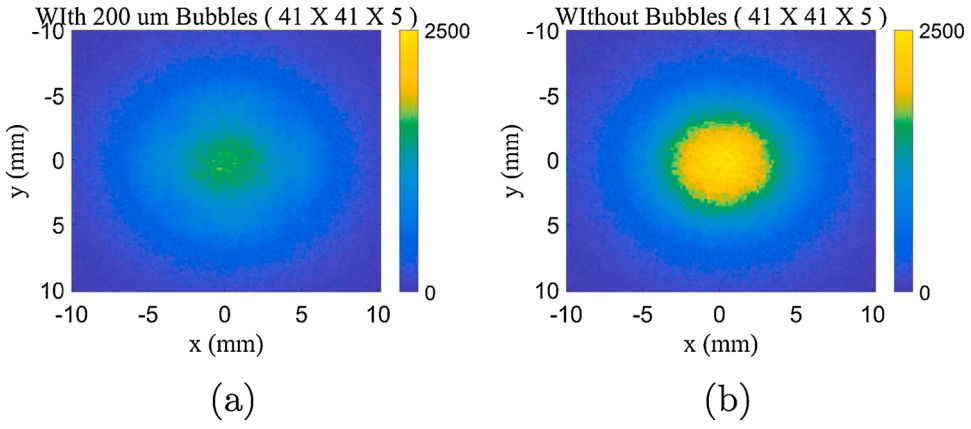

Fig. 8. The number of photons passed through a plane located at position B: (a) with air bubbles and (b) without bubbles.

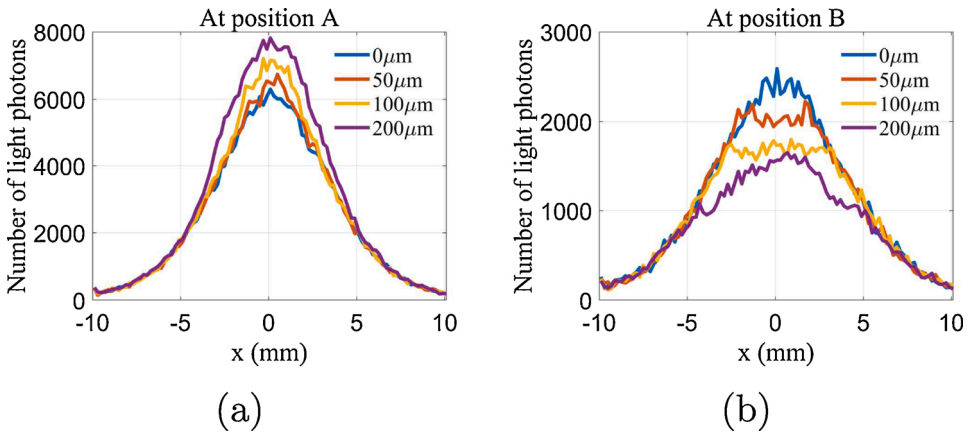

Fig. 9. The number of photons passed through a center line in planes described in Fig. 3: (a) at position A and (b) at position B.

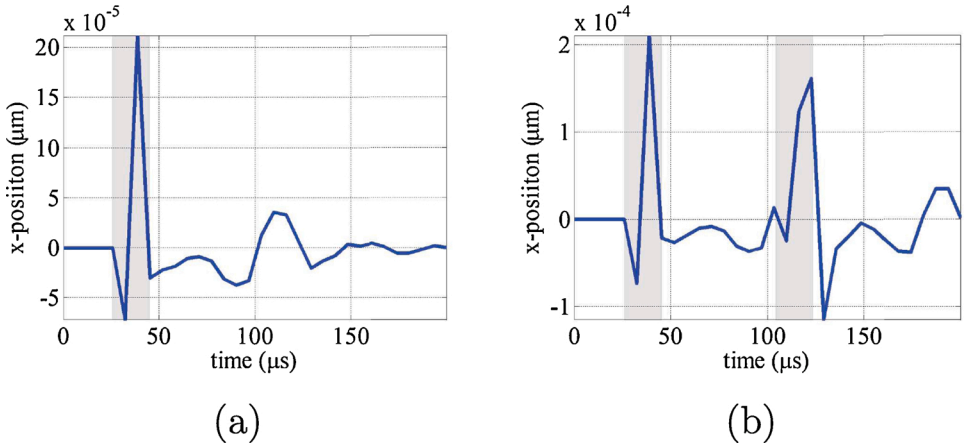

Fig. 10. Lateral displacement at point near the boundary of focal area, (a) 1 burst signal and (b) 2 burst signals. Shaded area indicates FUS pulse irradiation period.

$$x = \frac{2\pi r}{\lambda} \tag{5}$$

where r is the radius of spherical particle and λ is a wavelength of incident light. If the x value is less than 0.2, it means the Rayleigh scattering will occur and from 0.2 to 2000 represents the Mie scattering region. Therefore, because a wavelength of the light source used in our experiment was 637 nm, the size of air bubbles should be between diameter 40 nm and 400 μm, approximately. In this paper, effects by air bubbles with three different diameter, 50, 100 and 200 μm, were calculated.

Since air bubbles are generated in the focal volume of FUS, multi-layered air bubbles are modeled. Also, to avoid calculation error caused by the overlap between modeled air bubbles, a 10 μm gap between bubbles was applied.

Figs. 7 and 8 show the number of light photons that have passed through planes located at position A and position B illustrated in Fig. 3. In all cases, our calculation showed that the effect of reflection by air bubbles was greater than the effect of changes in the forward scattering rate by air bubbles. When there are air bubbles in the tissue, the number of photons in position A increased and the number of photons in position B decreased. Because the refractive index of the air bubbles is lower than the surrounding tissue, those calculation results show that photons are reflected in a backward direction. Therefore, the effect by the air bubbles alone cannot explain the observed increase of light transmission (Fig. 9).

Mechanical deformation of biological tissues by FUS can be another clue that can explain the light transmission enhancement. When the tissue is stretched by ultrasound, the density of scattering particles inside the stretched area will decrease. As the density decreases, the probability of scattering will decrease as well, leading to improved transmission. Therefore, if the change in the lateral displacement around the focal area can be calculated, the change in transmission also can be predicted.

Unfortunately, it was impossible to calculate according to the actual time range because our lateral displacement calculation was based on the finite time domain method. This type of calculation needs a huge amount of memory to calculate the actual time range. Therefore, our calculation was made in the shortened time range. However, it would not be unreasonable to look at the trend of changes in lateral displacement when FUS is applied. Fig. 10 shows lateral displacement near focal point caused by time-variant pressure at source points. Time variant shear stress was applied at the source point (Fig. 4(a)) and lateral displacement (displacement along x-axis) of acoustic particle located in the focal area (Fig. 4(c)) was calculated. Frequency of burst signal was set to be 0.515 MHz. All burst signals were composed of 10 cycles. Calculated time range was 200 μs which could contain 4 burst signals with different time gap between burst signals. Note that a positive lateral movement represents that the tissue has stretched.

4. Discussion

The increase of light transmission induced by FUS was observed in the rat brain tissue, as it was in chicken breast. [7] However, the transmittance of light increased by FUS was of relatively low intensity in the brain tissue than in the chicken breast. This is thought to be because

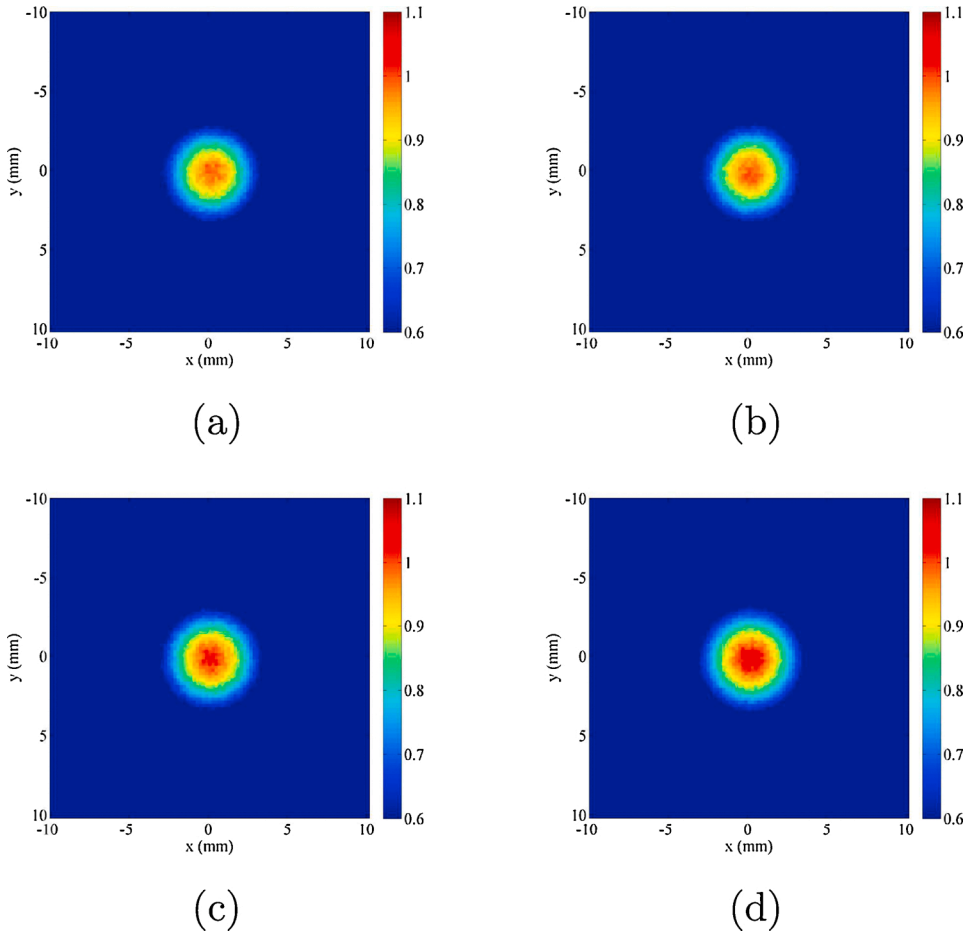

Fig. 11. Map of transmitted optical photons. (a) Original, (b) @*D*mean free path = 1%, (c) 5%, and (d) 10%.

the elasticity of the brain tissue is less than the elasticity of the chicken breast, based on the reason to be described later.

In this paper, changes in the density of scattering particles by the elastic shear wave and the modulation of scattering pattern caused by air bubbles via FUS, were considered as causes of the light transmission enhancement. Changes in optical properties by thermal effect were not taken into account because the tissue alteration caused by heat increases the absorption and scattering within the tissue [9].

Kim et al. insisted that air bubbles generated by FUS irradiation convert chicken breast tissue from the Rayleigh scattering region into the Mie scattering region; the existence of a threshold FUS power was suggested as one of the evidence. However, the enhancement of light transmission observed in FUS power was lower than Kim's findings [24]. The scattering anisotropy of the brain tissue approaches 0.9, indicating that the main optical scattering process inside the brain tissue is Mie scattering. Therefore, we need to check the effects of air bubbles on light transmission. According to Monte Carlo simulation results, air bubbles have been shown to reduce the transmittance of light. It was calculated that the transmission decreases even when there are air bubbles in water, although a simulated structure is slightly different from our case [25]. Basically, due to the occurrence of scattering prior to reaching the air bubbles, incident light is bound to have a variety of incident angles. Incident light having an angle of incidence more than a critical angle, determined by the difference between refractive index, is totally reflected. Therefore, there has to be some loss of light transmittance. And in our case, according to simulation results, that loss seems to be bigger than the gain of light transmittance by air bubbles. Therefore, we need another assumption to explain the enhancement.

Fundamentally, an ultrasonic wave is a travelling pressure disturbance that produces alternating compressions and expansions of the propagating medium [26]. As mentioned above, most biological tissues are nearly incompressible; therefore, alterations by the ultrasonic wave causes tissues to expand in a lateral direction [13,14]. Since the total number of cells in tissue is constant and the biological tissue is incompressible, the expansion of tissue indicates that the number of cells in unit volume decreased. Expansions and compressions in a lateral direction make an elastic shear wave in a medium. The ultrasound elastography uses signals caused by an elastic shear wave to generate images of elastic properties. Therefore, the existence of scientific reports about elastography of the brain also indicates that tissue expansion along the lateral direction could occur in brain tissue [27,28]. In this paper, we indirectly predicted the change in density through the lateral movement of the acoustic particle by the elastic wave. Although calculation was performed in a shorter time range than the actual time, the results show that the deformation by the first excitation by burst signal affects the deformation by subsequent excitation. Considering that lateral movement causes the stretching of tissues which decreases cell density and leads to an increase in transmitted light, these calculated results can explain the actual measurement (Fig. 6) of changing transmitted light intensity. From Fig. 10(a), it is shown that there exists a sudden motion of compression right after FUS pulse irradiation. And there also exists a relaxation process to return to the equilibrium position. Therefore, the decrease of transmitted intensity after FUS irradiation observed in Fig. 6 (c) could be explained by this motion of tissue compression. Considering that all experiments were performed with several minutes period and intensities before FUS irradiation of all experiments have little difference (Fig. 6(b)), it could be concluded that the previously observed decrease is temporary. Therefore, the relaxation phenomenon shown in

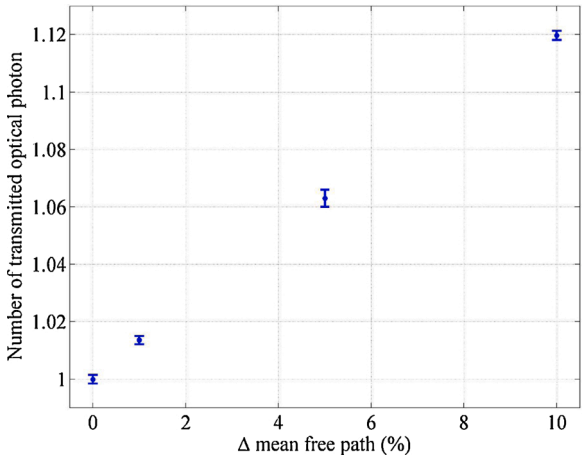

Fig. 12. Changes in total number of transmitted light photon.

the calculation result has also occurred. Since the second excitation occurred while the tissue was compressed due to the influence of the first FUS pulse, the increase in transmission intensity by the second excitation inevitably decreased compared to that by the first excitation. This phenomenon was observed both experiment (Fig. 6(a) and (b)) and calculation (Fig. 10(b)).

The reduced scattering coefficient is dependent on cell density [29]. The influence on the scattering parameters by changes in density was measured and reported [30]. Understandably, these lateral displacements are related to the elasticity of the material. Therefore, in the case of brain tissue which has lower elasticity compared to chicken breast, the tissue can be stretched more easily. The enhancement of transmission can also occur in the lower acoustic power compared to chicken breast.

An estimated change in cell density could be calculated by simple Monte-Carlo simulation. In our Monte-Carlo simulation, absorption and scattering length are used as important parameters. Considering that the sum of the absorption and scattering lengths is mean free path, which is inversely proportional to the density, the effect of change in cell density could be calculated by changing the values of the absorption and scattering lengths. Calculation results are shown in Figs. 11 and 12 . Comparing the calculation and the measurement results, it can be predicted that about 10% density change occurred. And assuming that there is no axial change in consideration of the incompressibility of the tissue, it can be predicted that the tissue has increased by 5% in the lateral direction.

Contrary to expectations, the fluctuation in peak pixel values in the 269 W/cm^2 was different from other results. It seems likely that this result is in fact due to the generation of air bubbles. According to Kim et al. [10], the power of 269 W/cm^2 is enough to generate cavitation air bubbles. Therefore, the underlying physics to explain the phenomenon in the power of 269 W/cm^2 is more complicated than other cases. However, we can still observe the phenomena in which the first excitation affects the second excitation.

5. Conclusions

Enhancement of light transmission in the rat brain caused by FUS irradiation is confirmed. We thought that both cavitation air bubbles and lateral movements in focal area could be the reason for this enhancement. Therefore, we carried out two types of simulation to calculate the effects of air bubbles and lateral movements on the enhancement. According to our calculation results, lateral movements are thought to be the cause of the enhancement while air bubbles play a negative role.

Unfortunately, our study had a limitation. The lateral movement caused by FUS was not accurately calculated or measured. The lack of computing power made calculations in the real-time domain impossible. However, the association between ultrasonic excitation events was observed in the calculation results of the lateral movement and the experimental results. The degree of lateral movement according to the experimental results was also predicted. Therefore, the measurement of lateral displacements by using other imaging technique will be our next step.

The limitation of penetration depth due to the scattering of biological tissues is one of the biggest hurdles of many light-based treatments and imaging techniques. In particular, many researchers have tried to overcome this limitation in photodynamic therapy (PDT), leading to the development of X-ray PDT and interstitial PDT. This phenomenon, as reported in this paper and preceeding papers, could be considered as another clue to overcome that limitation. Moreover, because this phenomenon is essentially based on reduction of scattering by biological media, the side effects on the surrounding normal tissue by scattered light photon will also be reduced.

Authors' contribution

Study concept and design: Seung Hee Han, Jaehyuk Kim and Won Seok Chang; experiment design and development: Jaehyuk Kim, Sung-Ho Lee, Jaewoo Shin, Chanho Kong and Won Seok Chang; simulation design and development: Jaehyuk Kim; data processing and analysis: Jaehyuk Kim; drafting of the manuscript: Jaehyuk Kim; revision of the manuscript for important intellectual content: Seung Hee Han and Jaewoo Shin; study supervision: Seung Hee Han.

Financial disclosure

None reported.

Conflict of interest

The authors declare no potential conflict of interests.

References

[1] R.J. Zemp, C. Kim, L.V. Wang, Ultrasound-modulated optical tomography with intense acoustic bursts, Appl. Opt. 46 (2007) 1615.
[2] A.P. Mosk, A. Lagendijk, G. Lerosey, M. Fink, Controlling waves in space and time for imaging and focusing in complex media, Nat. Photon. 6 (2012) 283–292.
[3] R. Horstmeyer, H. Ruan, C. Yang, Guidestar-assisted wavefront-shaping methods for focusing light into biological tissue, Nat. Photon. 9 (2015) 563–571.
[4] H. Yu, J. Park, K. Lee, J. Yoon, K. Kim, S. Lee, Y. Park, Recent advances in wavefront shaping techniques for biomedical applications, Curr. Appl. Phys. 15 (2015) 632–641.
[5] S. Rotter, S. Gigan, Light fields in complex media: mesoscopic scattering meets wave control, Rev. Mod. Phys. 89 (2017) 015005.
[6] I.M. Vellekoop, Feedback-based wavefront shaping, Opt. Express 23 (2015) 12189–12206.
[7] M. Kim, W. Choi, Y. Choi, C. Yoon, W. Choi, Transmission matrix of a scattering medium and its applications in biophotonics, Opt. Express 23 (2015) 12648–12668.
[8] J. SL, P. BW, Tutorial on diffuse light transport, J. Biomed. Opt. 13 (2008) 041302.
[9] R. JL, C. RO, R. RA, HIFU-induced changes in optical scattering and absorption of tissue over nine orders of thermal dose, Phys. Med. Biol. 63 (2018) 119–129.
[10] H. Kim, J.H. Chang, Increased light penetration due to ultrasound-induced air bubbles in optical scattering media, Sci. Rep. 7 (2017) 16105.
[11] S.L. Jacques, Optical properties of biological tissues: a review, Phys. Med. Biol. 58 (2013) R37.
[12] Z. Izadifar, P. Babyn, D. Chapman, Mechanical and biological effects of ultrasound: a review of present knowledge, Ultrasound Med. Biol. 43 (2017) 1085–1104.
[13] C. Zhang, D. Guo, H. Yin, D.C. Liu, X. Zhou, Ultrasound lateral displacement and lateral strain estimation using a two-step theory, J. Chem. Pharm. Res. 5 (2013) 332–337.
[14] L. Wang, Acoustic radiation force based ultrasound elasticity imaging for biomedical applications, Sensor 18 (2018) 2252.
[15] S.W. Cramer, C.C. Chen, Photodynamic therapy for the treatment of glioblastoma, Front. Surg. 6 (2020).
[16] F. Ultrasound Foundation, Focused Ultrasound Opening of the Blood-Brain Barrier for the Treatment of Parkinson's Disease, 2018 (Last accessed June 2020),

http://www.fusfoundation.org/images/pdf/Focused-Ultrasound-Foundation-Parkinsons-Disease-BBB-Workshop-2018-Report.pdf.
[17] A. J, et al., Recent Developments in GEANT4, Nucl. Instrum. Methods Phys. Res. A 835 (2016) 186–225.
[18] A. Dubois, C.-C. Chiang, F. Smekens, S. Jan, V. Cuplov, S. Palfi, K.-S. Chuang, S. Senova, F. Pain, Optical and thermal simulations for the design of optodes for minimally invasive optogenetics stimulation or photomodulation of deep and large cortical areas in non-human primate brain, J. Neural Eng. 15 (2018).
[19] G. Collaboration, Geant4 User's Guide for Application Developers, Version: geant4 10.3, 2016.
[20] G. Collaboration, Physics Reference Manual, 2017.
[21] A.N. Yaroslavsky, P.C. Schulze, I.V. Yaroslavsky, R. Schober, F. Ulrich, H.-J. Schwarzmaier, Optical properties of selected native and coagulated human brain tissues in vitro in the visible and near infrared spectral range, Phys. Med. Biol. 47 (2002) 2059–2073.
[22] B.E. Treeby, B.T. Cox, k-Wave: MATLAB toolbox for the simulation and reconstruction of photoacoustic wave fields, J. Biomed. Opt. 15 (2010) 021314.
[23] C.W. Barney, C.E. Dougan, K.R. McLeod, A. Kazemi-Moridani, Y. Zheng, Z. Ye, S. Tiwari, I. Sacligil, R.A. Riggleman, S. Cai, J.-H. Lee, S.R. Peyton, G.N. Tew, A. J. Crosby, Cavitation in soft matter, PNAS 117 (2019) 9157–9165.
[24] S.H. Han, W.S. Chang, J.H. Kim, The study of focused ultrasound effect to increase the penetration of light for photodynamic therapy of deeper tissue, Proc. SPIE 11079 (2019).
[25] G.E. Davis, Scattering of light by an air bubble in water, J. Opt. Soc. Am. 45 (1995) 7.
[26] W.D.O. Ultrasound Jr., - biophysics mechanism, Prog. Biophys. Mol. Biol. 93 (1–3) (2007) 212–255.
[27] F.-Y. Lay, P.-Y. Chen, H.-F. Cheng, Y.-M. Kuo, C.-C. Huang, Ex vivo evaluation of mouse brain elasticity using high-frequency ultrasound elastography, IEEE Trans. Biomed. Eng. 66 (2019).
[28] H. Tzschätzsch, B. Kreft, F. Schrank, J. Bergs, J. Braun, I. Sack, In vivo time-harmonic ultrasound elastography of the human brain detects acute cerebral stiffness changes induced by intracranial pressure variations, Sci. Rep. 8 (2018), https://doi.org/10.1038/s41598-018-36191-9.
[29] G.L. Cote', L.V. Wang, S. Rastegar, Biomedical Optics and Lasers, 3rd ed., Elsevier, 2012 https://doi.org/10.1016/C2009-0-19716-7.
[30] A. Haffner, P. Krauter, A. Kienle, Density-dependent determination of scattering properties of pharmaceutical tablets using coherent backscattering spectroscopy, Opt. Express 26 (2018).